Experimental Study on Global and Local Turbulent Premixed Flame Characteristics of Alcohols

J. Trabold*,, S. Walther*, S. Hartl*,***, A. Dreizler*, D. Geyer***

trabold@rsm.tu-darmstadt.de
*Thermodynamics, University of Applied Sciences, Darmstadt, Germany
** Reactive Flows and Diagnostics (RSM), TU Darmstadt, Germany
*** Simulation of reactive Thermo-Fluid Systems (STFS), TU Darmstadt

Abstract

Turbulent premixed flame characteristics are significant in technically relevant combustion processes. The here investigated fuels, belonging to the group of alcohols, are situated among the currently discussed biogenic fuels, which shall contribute to the emission reduction within the traffic sector. The aim of this experimental study is to discuss local and global flame characteristics to identify differences of the alcohols methanol, ethanol, 2-propanol and 2-butanol. The well-studied fuel methane is used as reference. All flames are stabilized on the novel Temperature Controlled Piloted Jet Burner (TCPJB), which incorporates an annular pilot flame and an air coflow. First, blow off Reynolds numbers for the different fuels are compared. Secondly, comparisons of CL images reveal differences in the global appearance of the flames. To detect the flame front and subsequently calculate the flame surface density (Σ) for varying bulk Reynolds (bulk Re) and equivalence ratios (ϕ), Planar Laser Induced Fluorescence (PLIF) of the OH molecule is used. The OH-PLIF images reveal significant differences between the fuels in the magnitude and distribution of Σ.

Introduction

In order to receive predictive modeling approaches for technical applications, turbulent combustion processes have to be assessed in detail, which requires comprehensive experimental data sets. Additionally, the potential of renewable energy sources is a central social issue and a topic of current research. In this contest, the turbulence-chemistry interaction and the local and global flame characteristics for fuels that are more complex than the widely investigated methane need to be investigated.

Velocity fields, spatially and temporarily resolved quantitative data of main species concentrations and temperature (Raman/Rayleigh scattering), as well as detailed information on the flame structure (e.g. OH-PLIF), are required for a more detailed understanding of flame-chemistry interaction and model validation. Effects of fuel variations on premixed flame structures were recently investigated by [1] for different C1 - C8 hydrocarbons using flame luminescence. [2] studied the flame structure of premixed flames of the alkanes methane, ethane and propane, stabilized

on a piloted Bunsen burner employing particle image velocimetry and Mie scattering. Still, detailed investigations on turbulent premixed flames of alcohol fuels in the gaseous phase are sparse and to the knowledge of the authors, a systematic analysis of global and local flame characteristics on the variation of liquid fuels is yet to be conducted.

The novel TCPJB was particularly developed to allow for the stabilization of gaseous and pre-vaporized liquid fuels over a wide range of equivalence ratios ϕ, mixture temperatures and bulk velocities. Within this work, the CL was captured to discuss flame appearance and to quantify global flame parameters, such as the flame height. Further, PLIF experiments were performed to obtain the flame surface density Σ. Flames were fueled by the four lowest chain-length alcohols methanol (CH_3OH), ethanol (C_2H_5OH), 2-propanol (C_3H_7OH) and 2-butanol (C_4H_9OH) were investigated at equivalence ratios ϕ varying from lean (ϕ=0.6) to rich (ϕ=1.5) conditions and operated at different bulk Reynolds numbers (bulk *Re*). Methane (CH_4) flames, at the same range of conditions, were employed to explore differences to a well-known gaseous fuel.

The capability to assess and describe the global and local flame structure of alcohols by means of the bulk blow-off Reynolds number, CL and the flame surface density gives a significant advance for understanding complex combustion processes for complex and alternative fuels.

Experimental Methodology

TCPJB System

A gear pump and Coriolis type mass flow controllers (MFCs, Bronkhorst, accuracy of 0.1 % FS) were employed to control the flow rate of the liquid fuels. The liquids were continuously vaporized over an evaporation matrix (ADrop, DV4), of which the temperature was limited to 573 K, to avoid thermal fuel decomposition. Further, the air flow was metered by a MFC and supplied to a temperature-controlled gas heater. Subsequently, the vaporized fuel and the heated air were mixed in a high shear static mixer. A second gas heater (ADrop NH3) was employed for bulk flows exceeding the thermal power of the first heater. Heated hoses between the gas heater/vaporizer system and the burner prevented partial condensation of the gaseous air/fuel mixture at cold spots. For the same reason, all flow conducting parts were temperature controlled by custom designed heating elements. An illustration of the burner nozzle section is given Fig. 1. The TCPJB consists of a central jet (inner diameter of D_i = 11.4 mm), surrounded by a co-annular pilot flame (D_i = 31.0 mm) and a homogeneous coflow (D_i = 260 mm) at 0.3 m/s air. The stainless steel tube temperature was controlled by three nozzle heaters (brown) up to 45 mm upstream of the burner exit. Thermocouples (type K) incorporated in the heating elements in

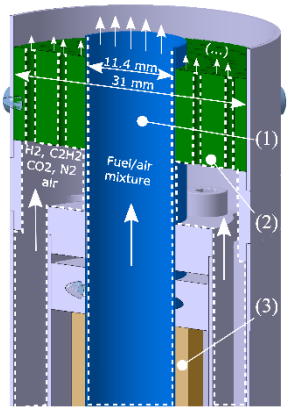

Figure 1. TCPJB jet and pilot area.

combination with PID controllers allowed for a temperature precision of about ±1 K up to temperatures of more than 400 K at the nozzle exit. As pilot flame, a co-annular slot, consisting of four rings holding 36 circular evenly distributed holes each, is utilized. Gas mixtures supplied to the pilot consisted of the five gases air, hydrogen, acetylene, carbon dioxide and nitrogen at ambient temperature. The gas composition was selected to match the C/H and C/O atom ratio, as well as the adiabatic temperature of the respective fuel/air mixture in the central jet at an equivalence ratio of $\phi = 0.7$. A constant pilot bulk velocity of $u_p = 1.0$ m/s was employed throughout all fuels.

Chemiluminescence imaging

Temporally averaged CL of the flames were captured using a Nikon D5600 and an 18-35 mm F1.8 Sigma lens at 31 mm with a pixel resolution of approximately 335 µm/pixel. The three major emitters in hydrocarbon flames within the sensitivity range of the experimental setup are CH* emitting around 431 nm, the Swan bands of C_2*, emitting between 430 nm and 650 nm, as well as the broadband emitting CO_2* [3]. Note that the experimental setup is insensitive in the wavelength region around 307 nm, where OH* radiates.

OH-PLIF imaging

OH-PLIF was used to image flame structures of the jet at six different axial positions. The laser beam emitted from a pulsed UV laser system at 283 nm and was formed into a 28 mm high and 0.2 mm thick sheet to excite the Q1(6) transition in the A-X (1-0) band. The OH fluorescence signal of a 24 x 32 mm^2 area was imaged onto a CCD camera (Imager E-lite, LaVision) using Intensified Relay Optics (High-speed IRO, LaVision). The pixel resolution of the detection system was 23 µm/pixel.

In a first step of data post-processing, images were background corrected. Next, the laser sheet intensity distribution was normalized using an in-situ averaged sheet profile [4]. The flame front was deduced to generate a binary burned/unburned image by tracking the highest gradient of OH [5]. Splines were fitted to recover the flame front. To deduce flame surface densities Σ as a measure of the mean reaction rate [6], flame lengths were determined in quadratic control areas. The size of the control areas was set to 0.2 x 0.2 mm^2. This was smaller than 20% of the smallest observed flame brush thickness (near the nozzle), but larger than the reaction zone thickness, as recommended by [7]. At fixed axial positions, cross sections of Σ are evaluated. Furthermore, Σ was integrated in radial direction to receive an axial distribution of Σ.

Laminar burning velocities

An in-house flame solver [8] was used to simulate one-dimensional adiabatic steady laminar premixed flames. The methane flames are modelled using the GRI30 mechanism by [9]. For methanol and ethanol the recently developed ELTE mechanism by [10] is used and for 2-propanol and 2-butanol the POLIMI/CRECK mechanism was chosen [11].

Results and Discussion

To explore global flame characteristics, CL images taken at lean, stoichiometric and rich conditions and at bulk *Re* of 18.000 are shown in Fig. 2.

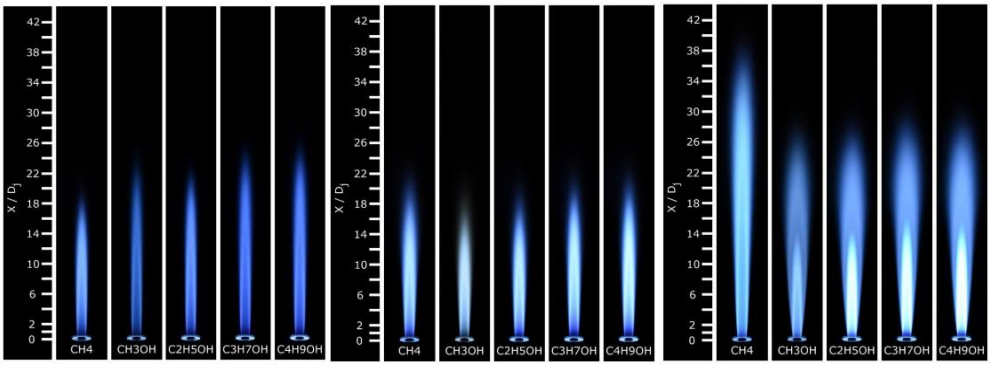

Figure 2. CL at bulk *Re* of 18000 and equivalence ratios ϕ of 0.8, 1.0, 1.5 (left to right).

At lean conditions (ϕ = 0.80), all flames are bluish, indicating mainly emissions from CH*. The luminosity is, over all axial positions, largest in the methane flame, which is in line with the largest CH mole fraction being located in stoichiometric methane flames [3]. At stoichiometric conditions, the flames appear more greenish for all fuels, which is due to C_2* emissions. At rich conditions (ϕ=1.5), a remarkable difference in between the alcohols and methane is visible. All alcohol flames show a bright, more greenish flame region, implying mostly C_2* emissions originating at rich conditions at lower axial distances, followed by a bluish flame region further downstream. The intensity of the CL within this lower axial region increases from methanol to 2-propanol, as the length of the C-chain in the molecules increases. Thus, a gain in the global fuel consumption rate in the lower axial region of the alcohol fueled rich flame is illustrated [1]. CH* emissions seem to be more prominent in the downstream flame region, as the color and the intensity substantially changes.

Fig. 3 shows the bulk Reynolds numbers *Re* at blow-off, the laminar burning velocities s_L and the normalized bulk velocities in dependency on the equivalence ratio ϕ. With respect to the blow off *Re*, all flames investigated show an increasing stability from lean towards rich conditions. *Re* of about 30000 and higher were reached at stoichiometric conditions and up to 60000 at rich conditions for the present pilot flame conditions. This demonstrates that the TCPJB configuration is well suited to study turbulence-chemistry interaction at technically relevant conditions. Further, global flame characteristics can be explored in dependency on s_L and the turbulent burning velocity. For lean conditions, the methane/air flames can be stabilized at higher bulk *Re* of the jet than the four alcohols. In contrast, flames based on the alcohol/air mixtures are more stable at rich conditions. Here, the stability of the flames is decreasing towards the one with the largest chain length. It is worth mentioning that methanol and ethanol show steeper gradients in stability than 2-propanol and 2-butanol.

The impact of s_L on the flame stability is illustrated in Fig. 3 c) by relating the bulk velocity at the nozzle exit at blow-off u_{bulk} to s_L. Alcohol fuels are grouped together at smaller u_{bulk}/s_L, while methane can withstand a larger u_{bulk}/s_L ratio in the present flow configuration. The difference in u_{bulk}/s_L is notably smaller within the alcohols than in between methane and the alcohols, revealing an impact of the fuel group on the flame stability. Fuels with the largest s_L showed the lowest stability. Further parameters relevant for flame stability will have to be investigated to address these impacts in more detail.

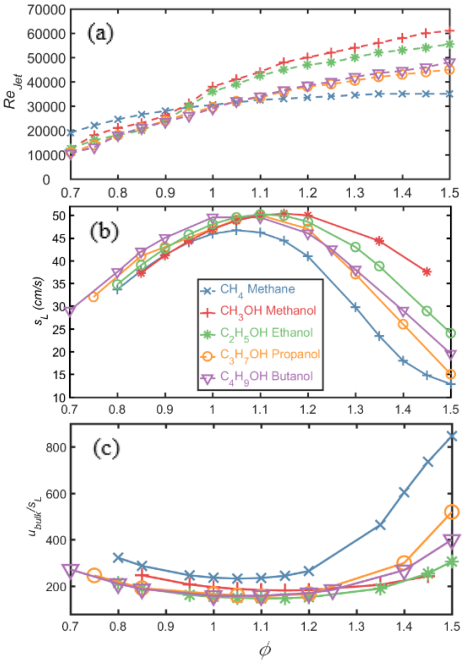

Figure 3. (a) Reynolds number at blow-off, (b) laminar burning velocity s_L and (c) normalized bulk velocity u_{bulk}/s_L over ϕ.

Lastly, the flame surface density Σ of flames with bulk Reynolds numbers of Re=18000 and equivalence ratios of ϕ=1.05 are discussed using results of OH PLIF measurements. Fig. 4 a) to c) show the evolution of Σ at three axial locations. At around x/D=1 (4a), the profile of Σ exhibits two distinct peaks, resulting from the plane of observation intersecting the flame centrally. At this location, Σ values are at maximum because flame intermittency is lowest. Further downstream, at x/D=5 (4b), the Σ profiles widen due to an increased flame brush thickness. Approaching the flame tip, the two peaks merge at around x/D=10 (4c). The integral of Σ along the radial direction is shown in Fig. 4 d), indicating the axial progression of mean reaction rates. Whereas methanol and ethanol flames reach their maximum at around x/D=7.5, methane, 2-propanol and 2-butanol peak around x/D=10. The gradient of Σ in axial direction is slightly larger for the alcohols, both up- and downstream the maximum peak. However, it should be considered that the methane flame was operated without preheating, using inlet temperatures of 293 K.

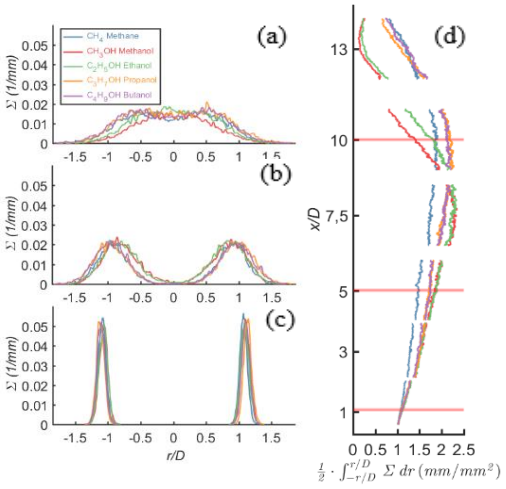

Figure 4. Radial distribution of flame surface density Σ at three heights ((a) to (c)) and integral Σ (d).

This reduces s_L (36.3 m/s instead of 46.7 m/s at 343 K) and reactivity is accordingly lower.

Conclusion

This experimental study discusses local and global flame characteristics of the alcohols methanol, ethanol, 2-propanol and 2-butanol. Significant differences between the fuels were found in the blow off Reynolds number, chemiluminescence images and the flame surface density. This serves as a indicator that flame stability, size and turbulence of the TCPJB flames are strongly dependent on the fuel type. In near future, experimental data will be analyzed with regards to influences of thermo-diffusive and hydrodynamic instabilities. Further, combined Raman- and Rayleigh measurements shall yield even more detail on the turbulence-chemistry interaction of alcohol flames, particularly of Ethanol.

Acknowledgements

We gratefully acknowledge financial support by the Deutsche Forschungsgemeinschaft (DFG) through GE 2523/2-1 and DR 374/17-1. A. Dreizler was financially supported by the Gottfried Wilhelm Leibniz-Preis (DFG). D. Geyer was financially supported by the ZFE of the Darmstadt University of Applied Sciences.

References

[1] Carbone, F., et al., “Comparative behavior of piloted turbulent premixed jet flames of C1-C8 hydrocarbons“, *Combustion and Flame*, 180:88-101 (2017).
[2] Tamadonfar, P. and Ö. L. Gülder "Experimental investigation of the inner structure of premixed turbulent methane/air flames in the thin reaction zones regime", *Comb. and Flame* 162(1):115-128 (2015).
[3] Kathrotia, T., et al. "Experimental and numerical study of chemiluminescent species in low-pressure flames", *Applied Physics B*, 107(3):571-584 (2012).
[4] Peterson, B. et al., “Early flame propagation in a SI engine measured with quasi 4D-diagnostics”, *Proc. Comb. Inst.*, 35:3829-3837 (2015).
[5] Nauert, A., „Laseroptische Untersuchungen an verdrallten Vormisch-flammen“, Technische Universität Darmstadt (2008).
[6] Bray, K. N. C., “Studies of the Turbulent Burning Velocity”, *Proceedings of the Royal Society A*, 431(1882):315-335 (1990).
[7] Donbar, J. and Driscol, J., “Reaction Zone Structure in Turbulent Nonpremixed Jet Flames - From CH-OH PLIF Images”, *Comb. and Flame*, 122:1–19 (2000).
[8] Zschutschke, A., et al.: “Universal Laminar Flame Solver (ULF)”, https://figshare.com/articles/ULF_code_pdf/5119855/2 (2017).
[9] Smith, G., P., et al., GRI30, in http://www.me.berkeley.edu/gri_mech/
[10] Olm, C., et al., ELTE, “Development of an Ethanol Combustion Mechanism Based on a Hierarchical Optimization Approach”, *International Journal of Chemical Kinetics*, 48:423-441 (2016).
[11] Frassoldati, R., et al., CRECK, *Comb. and Flame*, 159:2295-2311 (2012).